forests

MDPI

Article

Phenology-Based Method for Mapping Tropical Evergreen Forests by Integrating of MODIS and Landsat Imagery

Weili Kou [1,*], Changxian Liang [1], Lili Wei [1], Alexander J. Hernandez [2] and Xuejing Yang [1]

[1] School of Computer and Information, Southwest Forestry University, Kunming, Yunnan 650224 China; xnllcx@163.com (C.L.); lilywlwei@163.com (L.W.); yangxuejing0822@163.com (X.Y.)

[2] Remote Sensing and GIS Laboratories, Quinney College of Natural Resources, Utah State University, Logan, UT 84322, USA; alex.hernandez@usu.edu

* Correspondence: kwl@swfu.edu.cn; Tel.: +86-871-6386-3018

Academic Editor: Christian Ginzler

Received: 4 September 2016; Accepted: 20 January 2017; Published: 29 January 2017

Abstract: Updated extent, area, and spatial distribution of tropical evergreen forests from inventory data provides valuable knowledge for research of the carbon cycle, biodiversity, and ecosystem services in tropical regions. However, acquiring these data in mountainous regions requires labor-intensive, often cost-prohibitive field protocols. Here, we report about validated methods to rapidly identify the spatial distribution of tropical forests, and obtain accurate extent estimates using phenology-based procedures that integrate the Moderate Resolution Imaging Spectroradiometer (MODIS) and Landsat imagery. Firstly, an analysis of temporal profiles of annual time-series MODIS Normalized Difference Vegetation Index (NDVI), Enhanced Vegetation Index (EVI), and Land Surface Water Index (LSWI) was developed to identify the key phenology phase for extraction of tropical evergreen forests in five typical lands cover types. Secondly, identification signatures of tropical evergreen forests were selected and their related thresholds were calculated based on Landsat NDVI, EVI, and LSWI extracted from ground true samples of different land cover types during the key phenology phase. Finally, a map of tropical evergreen forests was created by a pixel-based thresholding. The developed methods were tested in Xishuangbanna, China, and the results show: (1) Integration of Landsat and MODIS images performs well in extracting evergreen forests in tropical complex mountainous regions. The overall accuracy of the resulting map of the case study was 92%; (2) Annual time series of high-temporal-resolution remote sensing images (MODIS) can effectively be used for identification of the key phenology phase (between Julian Date 20 and 120) to extract tropical evergreen forested areas through analysis of NDVI, EVI, and LSWI of different land cover types; (3) NDVI and LSWI are two effective metrics (NDVI $\geq$ 0.670 and 0.447 $\geq$ LSWI $\geq$ 0.222) to depict evergreen forests from other land cover types during the key phenology phase in tropical complex mountainous regions. This method can make full use of the Landsat and MODIS archives as well as their advantages for tropical evergreen forests geospatial inventories, and is simple and easy to use. This method is suggested for use with other similar regions.

Keywords: tropical evergreen forests; phenology features; remote sensing; MODIS; Landsat

1. Introduction

Global forests occupy 31% (4.0×10^7 km^2) of the total land area [1]. Tropical forests play a very important role in global carbon cycles, water and heat fluxes [2,3], biodiversity, and water and soil conservation, and produce half of the total Net Primary Production (NPP) of the world. However, across the world many tropical forests are being converted to farmlands, pastures, or other land cover

types driven by the increasing demand for food, energy, and economic activity, among others [4]. Moreover, in the past few decades over 80% of agricultural expansions occurred in tropical forest regions [4,5]. Tropical forest loss and degradation also affect different ecosystem services, which oftentimes lead to natural disasters. Accurate and up-to-date tropical forest maps are very important for tropical forest management and proper monitoring [6]. In some tropical areas, the increasing expansion of rubber plantations, to mention but one example, continually encroach tropical evergreen forests [7] in such a way that their areas are gradually decreasing. This situation causes a series of environmental problems, such as loss of biodiversity, and drought with such a magnitude that it becomes a hotspot issue to monitor the extent and change of forests in these areas that are prone to transition from primary forests to rubber plantations.

Producing timely and accurate tropical evergreen forest inventory data is very important for decision making and forest management. In this context, field measurements are also needed to validate biophysical attributes of the vegetation such as volume, carbon stocks, tree height, etc. However, traditional field sampling methods are limited in their application to tropical mountainous regions, and the accuracy of inventory data is constrained by the quality and quantity of the field samples [8]. Fortunately, remote sensing methods have evolved sufficiently to support forest inventories in large landscapes [9], which allows rapid, automatic, and periodical estimates of many forest inventory attributes [8] and can also help to improve the precision of forest area estimates [10].

Phenology is a vegetation feature that may be used to identify different characteristics such as plant growth, external shape forms, and colors. Phenology patterns are results of how vegetation adapts to the physical environment and climate over a long period of time, and is a very stable feature. Phenological differences among land cover types can be used for classification by means of remote sensing technology. Some terrestrial objects are difficult to be discerned by optical images since their spectral properties are very similar. Nevertheless, these objects can be easily distinguished in a specific period during the year given their particular phenological features during that same period of the year. For instance, evergreen forests and rubber plantations have very similar characteristics across environmental gradients in Southeast Asia. However, they can be easily distinguished by assessing their leaf-on and leaf-off phases, since rubber plantations are deciduous in winter but evergreen forests are not. In recent years, phenology-based methods have been used extensively in the field of vegetation monitoring by remote sensing technology, particularly for crops and plantations [11,12]. Combining satellite observations and ground truth data is an efficient way for land cover classification. Further, extraction of vegetation spatial distribution patterns based on long-term time series of satellite data is an important application of remote sensing technology.

The Landsat sensor has acquired global observation records for more than four decades, and can be freely accessed. This is an invaluable data source for local, regional, or global forest monitoring. Several Landsat-based global forest products have been generated, including a global map of mangroves [13], a 30-m global land cover map between 1999 to 2011 [14], and a global forest cover change map [15]. Landsat missions (Thematic Mapper TM, Enhanced Thematic Mapper /ETM+, and the Operational Land Imager /OLI) have been extensively used to map forests [1,15,16], but due to frequent cloud cover, high-quality images are hard to capture in tropical regions. Moderate Resolution Imaging Spectroradiometer (MODIS) imagery with a temporal resolution of eight days increases the chance to obtain quality data for target objects, and helps alleviate the shortage of other optical remote sensing sensors. MODIS is extensively used in Land Use and Land Cover Change (LULCC) studies including crop and plantation monitoring [5,17,18]. For instance, inter-annual time-series MODIS Enhanced Vegetation Index (EVI) and Short Wave Infrared (SWIR) have been efficiently used to identify rubber plantations in tropical mountainous regions [19].

In recent years, there has been an increasing interest by researchers worldwide to integrate imagery from multiple sensors. Landsat and Radar have been integrated to map rubber plantations in tropical regions [11], and MODIS and Landsat have been jointly used to monitor crops [20]. Hence, integration of multi-source remote sensing images is a growing research trend in many fields.

This study aims to integrate 500-m MODIS and 30-m Landsat to identify tropical evergreen forests based on vegetation phenology characteristics. MODIS with a high-revisit period (eight-days) enables capturing abundant and high-quality data for phenology-based time series analysis. Landsat data with fine spatial resolution (30m) can provide detailed spatial information and reduce mixing pixels to improve classification accuracy. Annual time-series MODIS Normalized Difference Vegetation Index (NDVI), EVI, and Land Surface Water Index (LSWI) are used to identify the key phenology phase that best fits tropical evergreen forest through analysis of differences in NDVI, EVI, and LSWI between evergreen forests and other typical land cover types. During the key phenology phase, indices and relevant thresholds were also identified through analysis and statistics of the values of NDVI, EVI, and LSWI for different land cover types based on 30-m Landsat images.

The objective of this study was to develop a phenology-based method for quickly extracting tropical evergreen forests for inventories and exploring their spatial distribution patterns by integrating MODIS and Landsat images across large scales. Mengyang, Jinuo, and Yunjinghong in Xishuangbanna, China were selected as the study area. The developed method is able to get accurate extent, areas, and spatial distribution for large-scale tropical evergreen forest inventory at 30-m spatial resolutions. These datasets can support basic inventory data for forestry planning and managing, ecosystem monitoring, regional land management, and other relevant research and applications.

2. Materials and Methods

2.1. The Study Area

This study was conducted in the Xishuangbanna Dai Nationality Autonomous Prefecture (Xishuangbanna), Yunnan, China. The total land area is 1.97×10^4 km^2, and the majority of the land (95%) is considered mountainous. The elevation ranges 344 m to 2,605 m above sea level. The total population is 1.14 million, with 69% dedicated to agricultural activities according to the Year Statistical Book of Xishuangbanna in 2010 [21]. The average annual precipitation is 1,550 mm, and the mean annual temperature is 21.7 °C [22]. Two major seasons are recognized in the study area: dry (from November to April), and rainy (from May to October). Rubber plantations cover more than 50% of the Yunnan Province, and are the second largest in China. Three major towns are included in the study area (Figure 1): Mengyang, Jinuo, and Yunjinghong. Due to the economic importance of natural rubber and agriculture, land use conflicts are common in the study area between these two classes and tropical evergreen forests.

2.2. Materials and Processing

NDVI, EVI, and LSWI are frequently used to stratify different land cover types. The key phenology phase—defined as an optimal time window for distinguishing tropical evergreen forests from other land cover types—was identified through analysis of annual time series created from multi-temporal eight-day-composites 500-m MODIS MOD09A1. Landsat imagery was acquired from the United States Geological Survey (USGS) server, and converted to surface reflectance using Landsat Ecosystem Disturbance Adaptive Processing System (LEDAPS) [23]. The rectified imagery was further processed using Fmask [24] to deal with clouds and shadows. During the key phenology phase, tropical evergreen forest was distinguished from other land cover types by using the improved Landsat imagery. A collection of photo-interpreted samples for algorithm training, time-series analysis, and results verification were created from geo-referenced field photos and Google Earth high quality imagery. This method is very effective and extensively used in current studies [11,25,26]. Google Earth high quality imagery can provide a reliable data source for interpreting and extracting samples (Figure 1B–F). Five typical land cover types (evergreen forests, rubber plantations, built-land, farmlands, and water bodies) were classified in the study area. NDVI, EVI, and LSWI are calculated using formulas (1)–(3). Land cover data of 500-m MODIS MCD12Q1 was used to compare with the resultant map of tropical evergreen forests [27].

$$NDVI = \frac{\rho_{NIR} - \rho_{red}}{\rho_{NIR} + \rho_{red}} \quad (1)$$

$$EVI = 2.5 \times \frac{\rho_{NIR} - \rho_{red}}{\rho_{NIR} + 6 \times \rho_{red} - 7.5 \times \rho_{blue} + 1} \quad (2)$$

$$LSWI = \frac{\rho_{NIR} - \rho_{SWIR}}{\rho_{NIR} + \rho_{SWIR}} \quad (3)$$

where ϱ_{NIR}, ϱ_{red}, ϱ_{MIR}, and ϱ_{blue} are the surface reflectance values of near infrared, red, shortwave-infrared, and blue bands in MODIS or Landsat images.

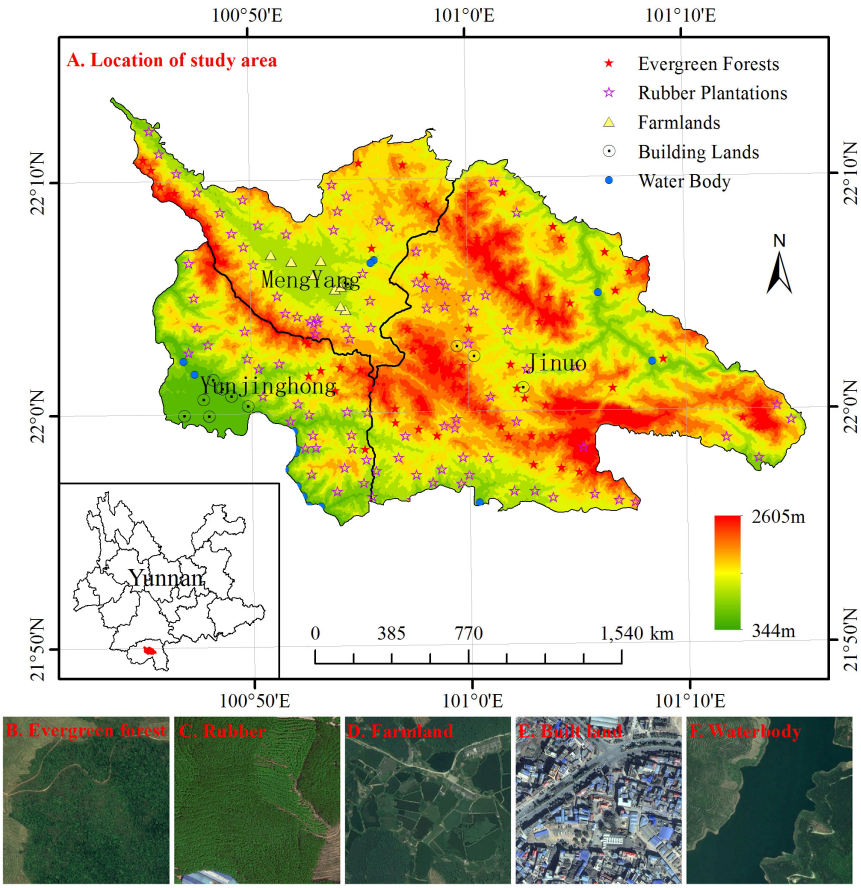

Figure 1. The study area location and samples for algorithm training and result verification. (**A**) is the location of three towns (Mengyang, Jinuo, and Yunjinghong) in Jinghong County Xishuangbanna, Yunnan, China, and spatial distributions for samples of five typical land cover types including evergreen forests, rubber plantations, farmlands, built-lands, and water bodies. They are created from geo-referenced field photos and Google Earth High quality imagery; (**B**–**F**) are high-resolution images of five typical land cover types from Google Earth.

2.3. Identifying the Key Phenology Phase

The key phenology phase is a relatively-fixed time window during which a particular vegetation type exhibits stable unique characteristics that are different from other land cover types. It is the optimal timing for distinguishing a kind of vegetation from others, and it was extensively used in previous studies [11,16,17]. Evergreen forests are stable ecosystems and have a strong resistance against influences from the physical environment (such as air temperature), whereas other land cover types (such as plantations and farmlands) are more susceptible to outside factors or mainly controlled by human activities. This phenomenon is generally reflected on the stability of annual

NDVI, EVI, and LSWI time-series curves of different land cover types. For instance, the NDVI curves of evergreen-forests are more stable than others.

Eight-day MODIS time-series have been extensively used to map paddy rice fields, forests, and plantations [17,28,29]. The key phenology phase can be identified through analysis of differences on annual time-series of MODIS NDVI, EVI, and LSWI of different land cover types. The fine temporal resolution is capable of capturing abundant, reliable, and continuous observation data in tropical regions, which supports annual time-series analysis for identification of the key phenology phase. Annual time-series profiles on NDVI, EVI, and LSWI of five typical land cover types were analyzed from temporal MODIS MOD09A1 between 2006 and 2014 based on samples created from geo-referenced field photos and Google Earth high resolution imagery. The method of creating these samples is very effective and extensively used in recent studies [11,16,26,30]. The phenological characteristics of different land cover types were used to discriminate evergreen forests from other land cover types during the key phenology phase. Considering the effects of mixing pixels caused by outside factors such as clouds, shadows, fragments, the minimum and maximum 3% were selected from 30-m Landsat NDVI, EVI, and LSWI time-series data of different land cover types [3]. This strategy was also used for analysis of the key phenology phase for extracting tropical evergreen forests.

2.4. Extracting Index Metrics and Relevant Thresholds

To extract tropical evergreen forests, high-quality Landsat 5 TM images captured on Julian Date 45 in 2010 were selected during the key phenology phase identified through analysis of MODIS annual time series. NDVI, EVI, and LSWI of evergreen forests, rubber plantations, farmlands, built-lands, and water bodies were extracted from Regions of Interests (ROIs) (Table 1) created from geo-referenced field photos and Google Earth high resolution images. These vegetation indices were evaluated by a statistical method to find an index combination with an ability to distinguish tropical forests from other land cover types.

Table 1. Regions of Interests (ROIs) created from geo-referenced field photos and Google Earth high resolution images for time-series analysis, algorithm training, and result verification in the study area.

ID	Land Cover Types	Pixels
1	Evergreen forests	26904
2	Rubber plantations	8392
3	Farmlands	268
4	Built-lands	785
5	Water bodies	538

This study's workflow for mapping tropical evergreen forests and exploring the spatial distribution is shown in Figure 2. First, annual time-series from 500-m MODIS images were analyzed to identify the key phenology phase; second, during the phenology phase, differences in 30-m Landsat NDVI, EVI, and LSWI of five typical land cover types were evaluated to select and determine the indices and relevant thresholds for extracting tropical evergreen forests; third, a 30-m map of tropical evergreen forest of the study area in 2010 was generated according to the indices and their thresholds determined above; fourth, the resultant map was verified using geo-referenced field photos and Google Earth high resolution imagery, and compared with MODIS MCD12Q1 land cover map for 2010; finally, the spatial distribution of evergreen forests at different elevation gradients was assessed based on a 90-m Digital Elevation Model (DEM) of the study area.

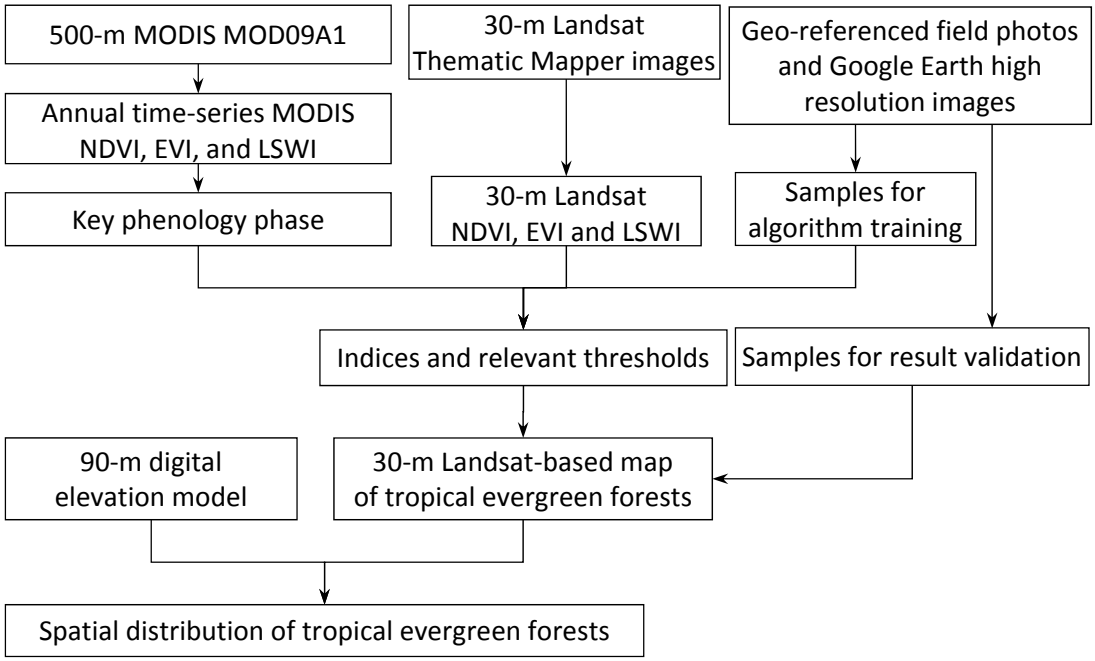

Figure 2. The technique workflow for mapping tropical evergreen forests. (1) A key phenology phase is selected based on analysis of annual time-series 500-m Moderate Resolution Imaging Spectroradiometer (MODIS) MOD09A1 Normalized Difference Vegetation Index (NDVI), Enhanced Vegetation Index (EVI), and Land Surface Water Index (LSWI) for different land cover types; (2) 30-m Landsat NDVI, EVI, and LSWI in the key phenology phase are evaluated to find an optimal combination of them for distinguishing tropical evergreen forests from other land cover types based on samples extracting from geo-referenced field photos and Google Earth high resolution images of the study area; (3) Based on (2), a 30-m map of tropic evergreen forests is generated based on Landsat Thematic Mapper (TM) imagery and verified by a confusion matrix built from samples created by the same method used above; (4) Spatial distribution of tropical evergreen forests is analyzed base on a 90-m digital elevation model.

3. Results

3.1. MODIS-Based Time-Series Analyses for Different Land Cover Types

Tropical evergreen forests can be distinguished from farmlands, built-lands, and water bodies on MODIS NDVI, EVI, and LSWI annual time series between Julian Dates 20 and 120 (Figure 3), so this time period was selected as the key phenology phase to extract evergreen forests. During this phase, the evergreen forest NDVI, EVI, and LSWI are higher than all other land cover types based on Landsat 5 TM images. This is because those evergreen forests have a strong ability to resist low air temperature in winter and spring (Julian Dates between 20 and 120), and the NDVI, EVI, and LSWI are relatively high. In addition, deciduous rubber plantations have a low canopy cover due to leaf-off conditions, and farmlands are not being cultivated at this time of year either.

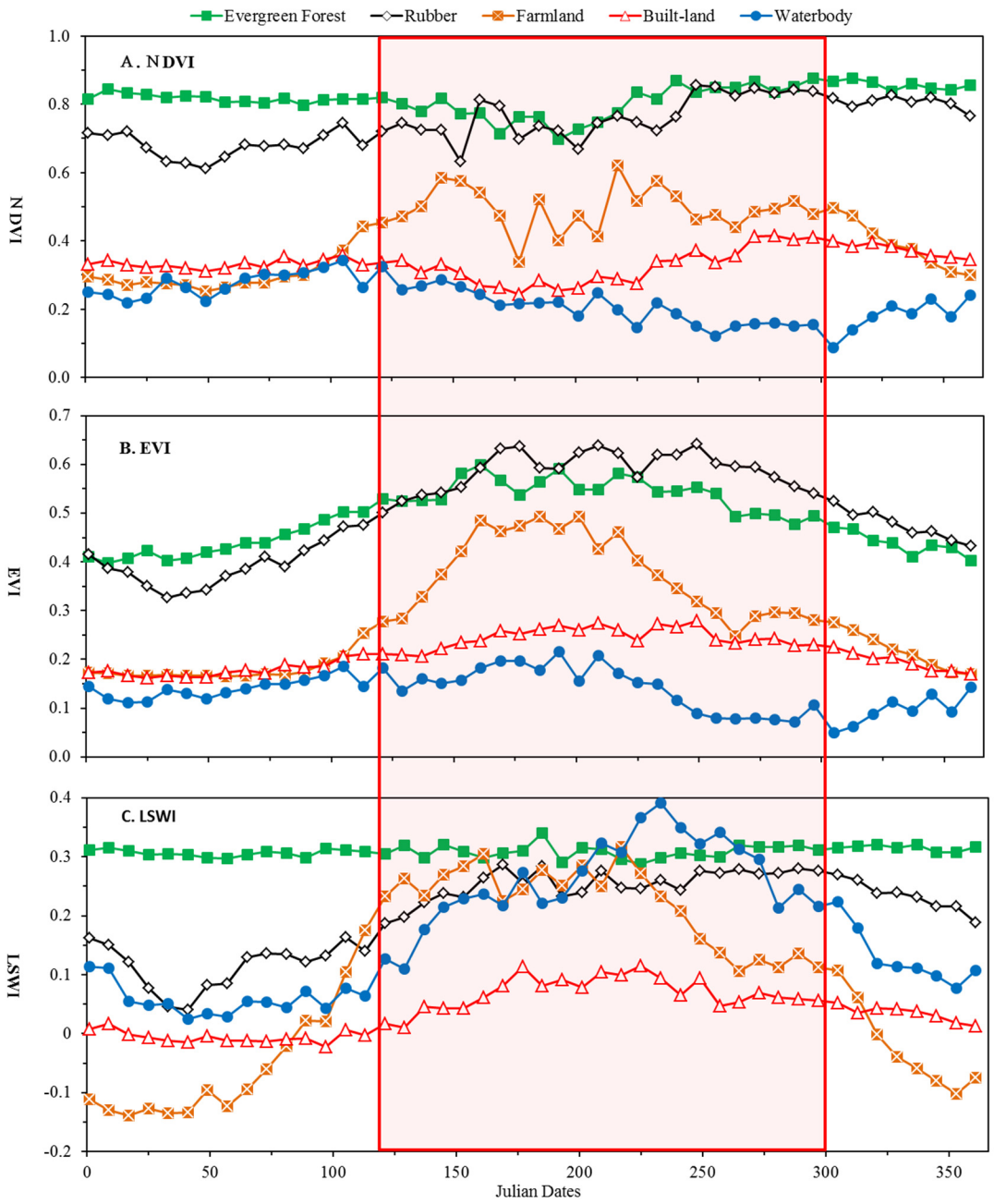

Figure 3. MODIS annual time-series analyses for different land cover types of the study area. Normalized Difference Vegetation Index (NDVI), Enhanced Vegetation Index (EVI), and Land Surface Water Index (LSWI) annual time series of five typical land cover types (evergreen forests, rubber plantations, farmlands, built-lands, and water bodies) were created from MODIS MOD09A1 between 2006 and 2014. Annual time-series profiles of NDVI (**A**); EVI (**B**); and LSWI (**C**) are separately analyzed to capture change information and rules of different land cover types of the study area. The area covered by red rectangle is the rainy season about from Julian Date 120 to 350 and the rest of the area represents the dry season in the study area.

3.2. Selection of Indices and Relevant Thresholds

NDVI of tropical evergreen forests is higher than deciduous rubber plantations, farmlands, built-lands, and water bodies, and LSWI is lower than water bodies and higher than farmlands, rubber plantations, and built-lands, respectively (Table 2). However, the evergreen forest EVI is prone to mix

with rubber plantations and farmlands. Therefore, Landsat 5 TM NDVI and LSWI were selected as the index metrics to extract tropical evergreen forests in the study area. Formulas (4)–(6) were designed to calculate thresholds of NDVI and LSWI. Since NDVI of tropical evergreen forests is far higher than other land cover types, just the minimum NDVI value needs to be calculated by formula (4), and the LSWI minimum and maximum can be calculated by formula (5) and (6). According to this, the thresholds are defined as NDVI $\geq$ 0.670 and 0.447 $\geq$ LSWI $\geq$ 0.222.

$$NDVI_{low} = NDVI_r + ((NDVI_e - NDVI_{ed}) - (NDVI_r + NDVI_{rd})/2 \quad (4)$$

$$LSWI_{lo} = LSWI_c + ((LSWI_e - LSWI_{ed}) - (LSWI_c + LSWI_{cd}))/2 \quad (5)$$

$$LSWI_u = LSWI_e + ((LSWI_w - LSWI_{wd}) - (LSWI_e + LSWI_{ed}))/2 \quad (6)$$

Here, NDVI, EVI, and LSWI were respectively extracted from Landsat 5 TM on Julian Date 45 in 2010. These are the average values of samples of five typical land cover types (rubber plantations, evergreen forests, farmlands, built-lands, and water bodies) in the study area. Subscript and superscript letters stand for relevant minimum and maximum values of NDVI, EVI, and LSWI; r, e, c, w, and r separately stand for values of different land cover types, and d, ed, cd, and wd for their relevant standard deviation. Figure 4 shows the statistical comparison of 30-m Landsat 5 TM NDVI, EVI, and LSWI of five typical land cover types. NDVI and LSWI are able to discern tropical evergreen forests from other land cover types, whereas EVI is unable to do so.

Table 2. NDVI, EVI, and LSWI of different land cover types of the study area of Xishuangbanna, Yunnan, China based on Landsat 5 TM images in 2010.

Land Cover Types	NDVI	EVI	LSWI
Evergreen Forests	0.743 ± 0.044	0.426 ± 0.076	0.312 ± 0.059
Rubber Plantations	0.563 ± 0.077	0.342 ± 0.069	0.053 ± 0.095
Farmlands	0.526 ± 0.067	0.337 ± 0.051	0.113 ± 0.079
Built-lands	0.341 ± 0.089	0.203 ± 0.055	−0.029 ± 0.084
Water bodies	0.015 ± 0.078	0.008 ± 0.034	0.618 ± 0.095

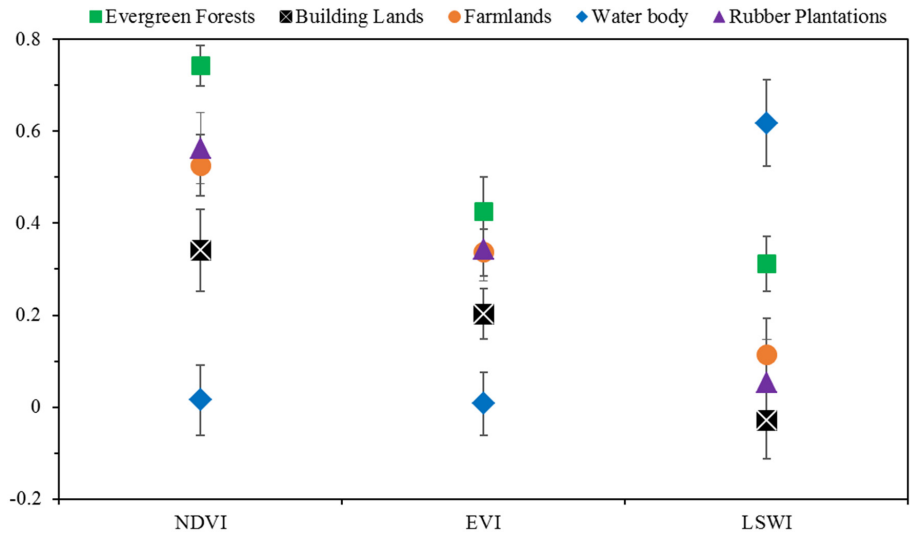

Figure 4. Signature analysis of the Normalized Difference Vegetation Index (NDVI), Enhanced Vegetation Index (EVI), and Land Surface Water Index (LSWI) for tropical evergreen forests, rubber plantations, farmlands, built-lands, and water bodies based on the Landsat Thematic Mapper (TM) 5 images between Julian Dates 20 and 120 in 2010 in the study area. Evergreen forests and other land cover types have distinctive values in NDVI and LSWI.

3.3. Landsat-Based Tropical Evergreen Forest Map of the Study Area in 2010

The output evergreen forest map (Figure 5) was verified by using the photo-interpreted locations described in the methods. To assess the map's accuracy a confusion matrix [11] was created. The samples included evergreen forests and other typical land cover types. According to the confusion matrix (Table 3), the overall accuracy is 92%; the user's and producer's accuracy of evergreen forests are 91% and 89% separately, and the accuracy of the other land cover types is 93% and 94%, respectively.

The spatial distribution of tropical evergreen forests in the output map for 2010 fits well to the false color (bands 5/4/3) composite Landsat 5 TM images-Julian Date 45 in 2010 (Figure 6). Furthermore, the resultant map (Figure 7B) was overlaid with the evergreen forests from the 500-m MODIS MCD12Q1 in 2010 (Figure 7A). The evergreen forest area of the Landsat-based output map is smaller than the one obtained from MODIS MCD12Q1. The possible reason for this is that mixed pixels are found due to the coarse spatial resolution and complex tropical mountain environment. For instance, some old rubber plantations have the similar phenology characteristics with evergreen forests and are misclassified.

Table 3. The accuracy assessment result of the tropical evergreen forest resultant map at 30-m spatial resolution in 2010 based on an error matrix. The overall accuracy is 92%.

	Class	Ground Truth Samples (pixels)		Total Class pixels	Producer's Accuracy
		Evergreen Forests	Others		
Classified results	**Evergreen forests**	3774	353	4127	91%
	Others	373	3843	4425	93%
Total ground truth pixels		4238	6240	10,478	
User's accuracy		89%	94%		

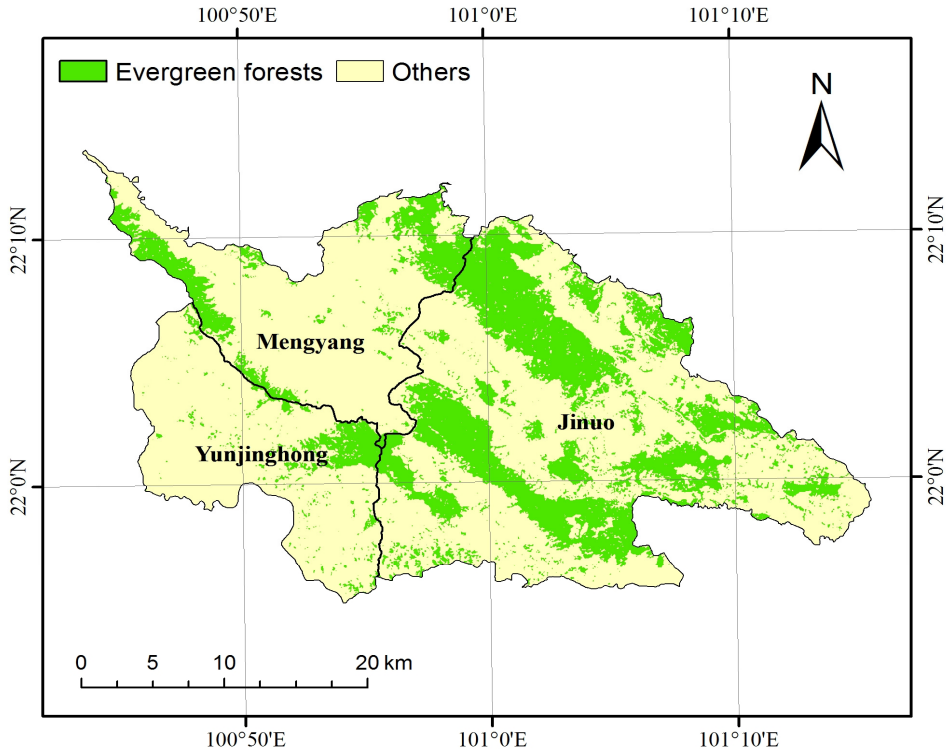

Figure 5. The 30-m Landsat-based map of tropical evergreen forest of the study area in Xishuangbanna, Yunnan, China in 2010.

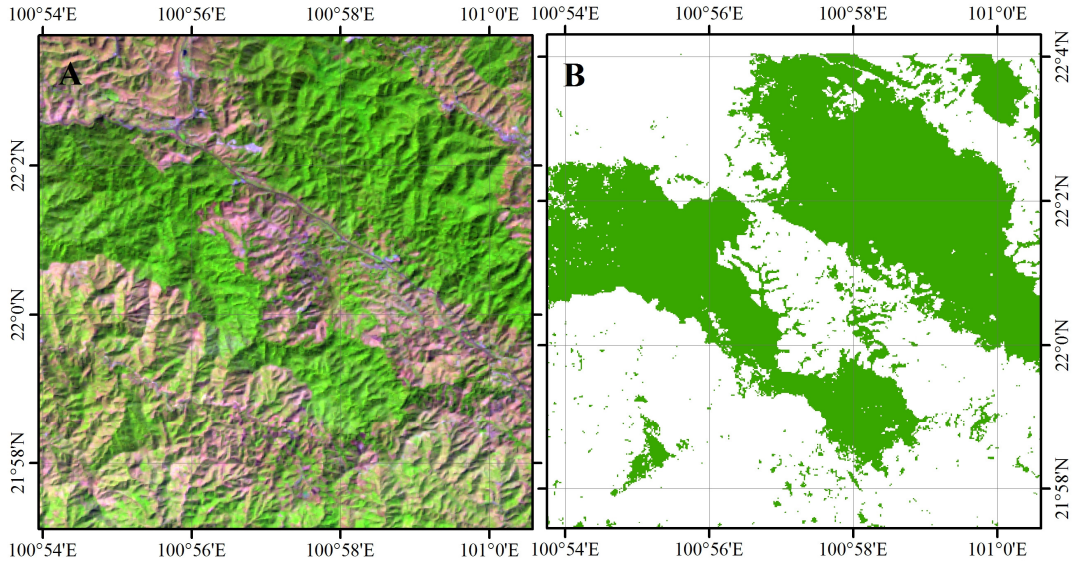

Figure 6. The resultant map is compared with the 30-m Landsat 5 Thematic Mapper (TM) image on the Julian Date 45 in 2010. The evergreen forest shows as green on the composite Landsat 5 TM image (**A**) combined as false color (bands 5/4/3); and (**B**) is the 30-m Landsat-based resultant map of tropical evergreen forests in the study area in 2010.

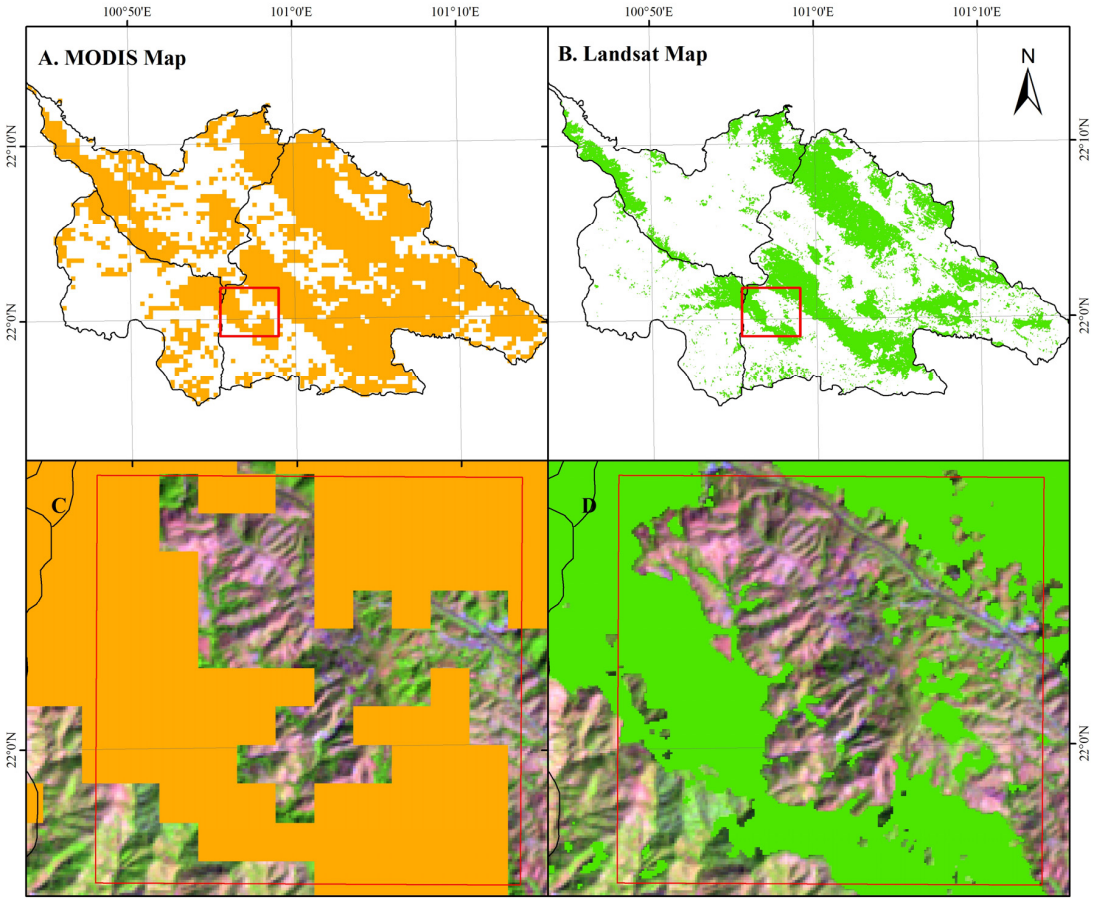

Figure 7. Comparison of eight-day 500-m MODIS MCD12Q1 (**A**) and the 30-m Landsat resultant map (**B**) in 2010. The two zoom-out windows below display the detailed information of MODIS MCD12Q1 (**C**) and the resultant map of 30-m Landsat 5 TM (**D**).

3.4. Distribution of Evergreen Forests on Different Elevation Gradients

The distribution of tropical evergreen forests of the resultant map was analyzed by resampled 30-m DEM of the study area (Figure 8). The results show that tropical evergreen forests are majorly distributed in a narrow elevation range between 900 m and 1400 m, and few forest patches are found in lower (<900 m) and higher elevations (>1400 m).

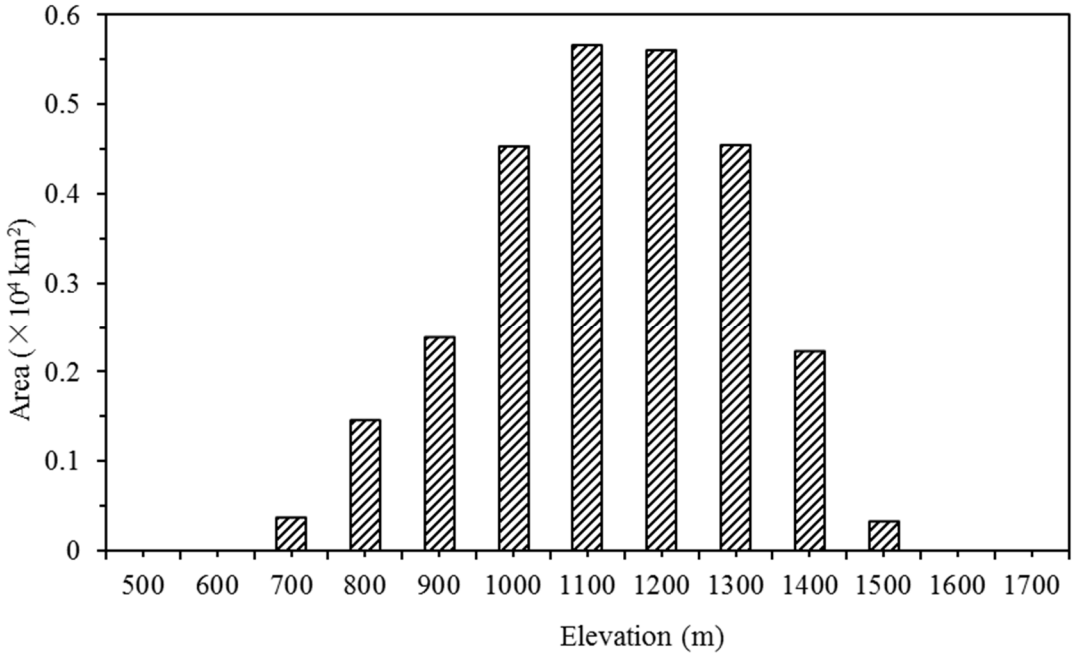

Figure 8. Distribution of tropical evergreen forests on different elevation gradients based on resampled 30-m digital elevation model in the study area of Xishuangbanna, Yunnan, China in 2010.

4. Discussion

The results from this study reinforces the notion that fine temporal resolution annual time series (eight-day MODIS) are capable of distinguishing the key phenology phase to extract tropical evergreen forests in tropical regions. These time-series can provide abundant and highly-reliable basic scientific data. In this particular case, it was established that the phenology phase can be identified from Julian Dates 20–120, and that this important phenological signature can be effectively used to extract tropical evergreen forests through analysis of NDVI, EVI, and LSWI of different land cover types. In tropical regions, cloud-free observations are difficult to get due to frequent clouds and shadows. Nevertheless, having coarser spatial resolution with high-temporal-resolution sensors can increase the possibility of getting good quality remote sensing images. This approach takes advantages of the high-revisit characteristics of the MODIS sensor, which increase the possibility of capturing good quality images from optical sensors. Annual MODIS time-series have been used in previous research [3,12,31–33], and most of them are not in tropical mountainous regions. It should be mentioned, however, that the coarse spatial resolution (500 m) may produce some inaccurate results from mixing pixels of small-area land cover types, such as narrow rivers.

Distinguishing tropical evergreen forest and deciduous forest is a challenge in Southeast Asia based on optical remote sensing images. The phenology-based method used in several studies is very useful for mapping paddy rice fields [17] and rubber plantations [11]. In this study, the key phenology phase was used to distinguish tropical evergreen forests in mountainous regions. Vegetation in different growth stages exhibits various distinct characteristics in terms of forms, color, and shape. Spectral reflectance characteristics of different land cover types are similar in some phases and different in others. For instance, as it was shown in this paper, annual time-series MODIS NDVI of evergreen

forests is higher than other land cover types on Julian Dates between 20 and 120 (Figure 3). Based on this finding, evergreen forests were distinguished from other land cover types in tropical mountainous regions based on 30-m Landsat 5 TM images. This study demonstrates that highly-temporal time-series are useful in observing key phenology phase for mapping a certain land cover type in certain time periods in tropical humid regions.

The vegetation indices and related thresholds were keys for accurately mapping evergreen forests. Easy to carry out and to understand statistical methods are often used to choose indices and compute related threshold values based on samples of different land cover types. At present, there is a lack of efficient methods for choosing indices and computing related thresholds for quickly and efficiently distinguishing evergreen forests in tropical regions of Southeast Asia. This study found that 30-m Landsat NDVI and LSWI are two efficient indices for distinguishing evergreen forests in these tropical environments. A general method (formulae (4)–(6)) for calculating related thresholds by a statistical method has been described and provided in this paper. Thirty-meter Landsat NDVI and LSWI are two effective metrics (NDVI $\geq$ 0.670 and 0.447 $\geq$ LSWI $\geq$ 0.222) to discern tropical evergreen forests for inventories from other land cover types during the key phenology phases in tropical complex mountainous regions. In the past few decades, driven by urban and economic developments, tropical forests were substantially converted to farmlands and rubber plantations in Xishuangbanna, Yunnan China. However, an accurate spatial distribution of the remaining forests was hard to determine in this region. This study generated an accurate evergreen forest map (Figure 5) of the study area and explored the forests' distribution across an elevation gradient (Figure 8). It was found that evergreen forest is mainly distributed in a very narrow range (900 m–1400 m) of elevation. A possible reason for this is that farmlands and plantations mainly dominate the low-elevation regions, and the high-elevation regions are cultivated for planting economic crops such as tea plants. This may lead to the loss of vertical forest diversity and biodiversity, and threatens the local ecosystem, biodiversity, and environment. This implies that these ecosystems are susceptible to a land cover transition, thus local governments need to take action for their protection. In this paper, a phenology-based automated mapping algorithm was shown to perform well in tropical mountainous regions. The study explored the extent, areas, and spatial distribution of tropical evergreen forest in this region of South Asia, and evaluated the efficiency and applicability of the method.

Additionally, samples created from geo-referenced photos and high resolution images of Google Earth provide reliable basic data for algorithm training and result validation. These geo-referenced filed photos are firstly transferred into xml files and then linked with high resolution imagery of Google Earth, in which samples are visually and interactively created.

5. Conclusions

This study attempted to develop a novel phenology-based method to map tropical evergreen forests by integrating 30-m Landsat and eight-day 500-m MODIS remotely sensed images during a key phenology phase. The developed and verified protocol is simple yet effective. Integration of multi-source remote sensing data with different spatial and temporal resolutions proved satisfactory to obtain accurate estimates of the extent, areas, and spatial distribution of tropical evergreen forest in Southeast Asia. Additionally, identification of the key phenology phase is very important to distinguish evergreen forest from other land cover types based on vegetation indices including NDVI, EVI, and LSWI. The assessment of the spatial distribution of evergreen forest across the elevation gradient showed that the remaining forest is fragmented and needs to be protected. Additionally, the study suggests that the local government can compensate farmers to encourage them to farm in low-elevation gradients and to withdraw from ecosystem-weak regions in high-elevation gradients, for example, by establishing guidelines for planting rubber trees below 950 m. This study also illustrates that our output map can provide more detailed and accurate spatial information than MODIS MCD12Q1. However, there are still some uncertainties in the methods due to the relatively coarse temporal and spatial resolution of remote sensing data and the influence of frequent clouds, shadows, and

aerosols. The integration with other sources (such as microwave, lidar, and optical) with finer spatial and temporal resolution may be tested in future studies to improve the presented methods for the extraction of tropical evergreen forests.

Acknowledgments: This work was supported by the National Natural Science Foundation of China (No. 31400493) and the Research Center of Kunming Forestry Information Engineering Technology (Grant No. 2015FIB04). We thank three anonymous peer reviewers for their helpful and valuable suggestions and comments to improve this manuscript.

Author Contributions: Weili Kou conceived and designed the experiments; Changxian Liang, Lili Wei, and Xuejing Yang performed the experiments; Weili Kou and Alexander J. Hernandez wrote the paper. All co-authors assisted the lead author in writing and revising the manuscript.

Conflicts of Interest: The authors declare no conflicts of interest.

References

1. Qin, Y.; Xiao, X.; Dong, J.; Zhang, G.; Shimada, M.; Liu, J.; Li, C.; Kou, W.; Moore, B., III. Forest cover maps of china in 2010 from multiple approaches and data sources: Palsar, landsat, modis, fra, and nfi. *ISPRS J. Photogramm. Remote Sens.* **2015**, *109*, 1–16. [CrossRef]
2. Pongratz, J.; Reick, C.H.; Raddatz, T.; Claussen, M. Biogeophysical versus biogeochemical climate response to historical anthropogenic land cover change. *Geophys. Res. Lett.* **2010**, *37*, 162–169. [CrossRef]
3. Qin, Y.; Xiao, X.; Dong, J.; Zhang, G.; Roy, P.S.; Joshi, P.K.; Gilani, H.; Murthy, M.S.R.; Jin, C.; Wang, J. Mapping forests in monsoon asia with alos palsar 50-m mosaic images and modis imagery in 2010. *Sci. Rep.* **2016**, *6*, 1–10. [CrossRef] [PubMed]
4. Gibbs, H.K.; Ruesch, A.S.; Achard, F.; Clayton, M.K.; Holmgren, P. Tropical forests were the primary sources of new agricultural land in the 1980s and 1990s. *Proc. Natl. Acad. Sci. USA* **2010**, *107*, 16732–16737. [CrossRef] [PubMed]
5. Kwak, Y.; Park, J.; Fukami, K. Near real-time flood volume estimation from modis time-series imagery in the indus river basin. *IEEE J. Sel. Top. Appl. Earth Obs. Remote Sens.* **2014**, *7*, 578–586. [CrossRef]
6. Hansen, M.C.; Stehman, S.V.; Potapov, P.V. From the cover: Quantification of global gross forest cover loss. *Proc. Natl. Acad. Sci. USA* **2010**, *107*, 8650–8655. [CrossRef] [PubMed]
7. Yi, Z.F.; Cannon, C.H.; Chen, J.; Ye, C.X.; Swetnam, R.D. Developing indicators of economic value and biodiversity loss for rubber plantations in Xishuangbanna, southwest China: A case study from menglun township. *Ecol. Indic.* **2014**, *36*, 788–797. [CrossRef]
8. Liang, X.; Kankare, V.; Hyyppä, J.; Wang, Y.; Kukko, A.; Haggrén, H.; Yu, X.; Kaartinen, H.; Jaakkola, A.; Guan, F.; et al. Terrestrial laser scanning in forest inventories. *ISPRS J. Photogramm. Remote Sens.* **2016**, *115*, 63–77. [CrossRef]
9. McRoberts, R.E.; Tomppo, E.O. Remote sensing support for national forest inventories. *Remote Sens. Environ.* **2007**, *110*, 412–419. [CrossRef]
10. McRoberts, R.E.; Wendt, D.G. Using a land cover classification based on satellite imagery to improve the precision of forest inventory area estimates. *Remote Sens. Environ.* **2002**, *81*, 36–44. [CrossRef]
11. Dong, J.; Xiao, X.; Chen, B.; Torbick, N.; Jin, C.; Zhang, G.; Biradar, C. Mapping deciduous rubber plantations through integration of palsar and multi-temporal landsat imagery. *Remote Sens. Environ.* **2013**, *134*, 392–402. [CrossRef]
12. Sakamoto, T.; Yokozawa, M.; Toritani, H.; Shibayama, M.; Ishitsuka, N.; Ohno, H. A crop phenology detection method using time-series modis data. *Remote Sens. Environ.* **2005**, *96*, 366–374. [CrossRef]
13. Giri, C.; Ochieng, E.; Tieszen, L.L.; Zhu, Z.; Singh, A.; Loveland, T.; Masek, J.; Duke, N. Status and distribution of mangrove forests of the world using earth observation satellite data. *Glob. Ecol. Biogeogr.* **2011**, *20*, 154–159. [CrossRef]
14. Gong, P.; Wang, J.; Yu, L.; Zhao, Y.; Zhao, Y.; Liang, L.; Niu, Z.; Huang, X.; Fu, H.; Liu, S. Finer resolution observation and monitoring of global land cover: First mapping results with landsat tm and etm+ data. *Int. J. Remote Sens.* **2012**, *34*, 2607–2654. [CrossRef]
15. Hansen, M.C.; Potapov, P.V.; Moore, R.; Hancher, M.; Turubanova, S.A.; Tyukavina, A.; Thau, D.; Stehman, S.V.; Goetz, S.J.; Loveland, T.R.; et al. High-resolution global maps of 21st-century forest cover change. *Science* **2013**, *342*, 850–853. [CrossRef] [PubMed]

16. Kou, W.; Xiao, X.; Dong, J.; Gan, S.; Zhai, D.; Zhang, G.; Qin, Y.; Li, L. Mapping deciduous rubber plantation areas and stand ages with palsar and landsat images. *Remote Sens.* **2015**, *7*, 1048–1073. [CrossRef]
17. Xiao, X.; Boles, S.; Liu, J.; Zhuang, D.; Frolking, S.; Li, C.; Salas, W.; Iii, B.M. Mapping paddy rice agriculture in southern china using multi-temporal modis images. *Remote Sens. Environ.* **2005**, *95*, 480–492. [CrossRef]
18. Liu, X.; Feng, Z.; Jiang, L.; Zhang, J. Rubber plantations in xishuangbanna: Remote sensing identification and digital mapping. *Resour. Sci.* **2012**, *34*, 1769–1780.
19. Senf, C.; Pflugmacher, D.; Linden, S.V.D.; Hostert, P. Mapping rubber plantations and natural forests in Xishuangbanna (southwest China) using multi-spectral phenological metrics from modis time series. *Remote Sens.* **2013**, *5*, 2795–2812. [CrossRef]
20. Xie, D.; Sun, P.; Zhang, J.; Zhu, X. Autumn Crop Identification Using High-Spatial-Temporal Resolution Time Series Data Generated by Modis and Landsat Remote Sensing Images. In Proceedings of the IGARSS 2014—2014 IEEE International Geoscience and Remote Sensing Symposium, Quebec City, QC, Canada, 13–18 July 2014; pp. 2118–2121.
21. Editorial Board of the Year Statistical Book of Xishuangbanna. *The Year Statistical Book of Xishuangbanna in 2010*; Dehong Nationalities Publishing House: Dehong, China, 2011.
22. Lü, X.T.; Yin, J.X.; Tang, J.W. Diversity and composition of understory vegetation in the tropical seasonal rain forest of Xishuangbanna, SW China. *Rev. Biol. Trop.* **2011**, *59*, 455–463. [CrossRef] [PubMed]
23. Masek, J.G.; Vermote, E.F.; Saleous, N.; Wolfe, R.; Hall, F.G.; Huemmrich, K.F.; Gao, F.; Kutler, J.; Lim, T.K. *Ledaps Calibration, Reflectance, Atmospheric Correction Preprocessing Code, Version 2*; ORNL Distributed Active Archive Center: Oak Ridge, TN, USA, 2013.
24. Zhu, Z.; Woodcock, C.E. Object-based cloud and cloud shadow detection in landsat imagery. *Remote Sens. Environ.* **2012**, *118*, 83–94. [CrossRef]
25. Dong, J.; Xiao, X.; Sheldon, S.; Biradar, C.; Xie, G. Mapping tropical forests and rubber plantations in complex landscapes by integrating palsar and modis imagery. *ISPRS J. Photogramm. Remote Sens.* **2012**, *74*, 20–33. [CrossRef]
26. Lu, N.; Hernandez, A.J.; Ramsey, R.D. Land cover dynamics monitoring with landsat data in kunming, china: A cost-effective sampling and modelling scheme using google earth imagery and random forests. *Geocarto Int.* **2014**, *30*, 186–201. [CrossRef]
27. Friedl, M.A.; Sulla-Menashe, D.; Tan, B.; Schneider, A.; Ramankutty, N.; Sibley, A.; Huang, X. Modis collection 5 global land cover: Algorithm refinements and characterization of new datasets. *Remote Sens. Environ.* **2010**, *114*, 168–182. [CrossRef]
28. Liu, F.J.; Huang, C.; Pang, Y.; Li, M.; Song, D.X.; Song, X.P.; Channan, S.; Sexton, J.O.; Jiang, D.; Zhang, P. Assessment of the three factors affecting myanmar's forest cover change using landsat and modis vegetation continuous fields data. *Int. J. Digit. Earth* **2016**, *9*, 1–24. [CrossRef]
29. Setiawan, Y.; Pawitan, H.; Prasetyo, L.B.; Lubis, M.I.; Parlindungan, M.; Nurdiana, A. Characterizing spatial distribution and environments of sumatran peat swamp area using 250 m multi-temporal modis data. *Procedia Environ. Sci.* **2016**, *33*, 117–127. [CrossRef]
30. Dong, J.; Xiao, X. Evolution of regional to global paddy rice mapping methods: A review. *ISPRS J. Photogramm. Remote Sens.* **2016**, *119*, 214–227. [CrossRef]
31. Wardlow, B.D.; Egbert, S.L.; Kastens, J.H. Analysis of time-series modis 250 m vegetation index data for crop classification in the U.S. Central great plains. *Remote Sens. Environ.* **2007**, *108*, 290–310. [CrossRef]
32. Dorjsuren, M.; Liou, Y.-A.; Cheng, C.-H. Time series MODIS and in situ data analysis for mongolia drought. *Remote Sens.* **2016**, *8*, 509. [CrossRef]
33. Zeng, L.; Wardlow, B.D.; Wang, R.; Shan, J.; Tadesse, T.; Hayes, M.J.; Li, D. A hybrid approach for detecting corn and soybean phenology with time-series modis data. *Remote Sens. Environ.* **2016**, *181*, 237–250. [CrossRef]